Korean J. Chem. Eng., **31**(6), 1049-1056 (2014)
DOI: 10.1007/s11814-014-0021-7

pISSN: 0256-1115
eISSN: 1975-7220

Extraction separation of toluene/cyclohexane with hollow fiber supported ionic liquid membrane

Fan Zhang, Wei Sun, Junteng Liu, Weidong Zhang, and Zhongqi Ren[†]

Beijing Key Laboratory of Membrane Science and Technology,
Beijing University of Chemical Technology, Beijing 100029, P. R. China

(*Received 12 October 2013 • accepted 14 January 2014*)

Abstract−A supported liquid membrane with ionic liquid was used for the separation of toluene/cyclohexane. The interactions of ionic liquid with toluene and cyclohexane were calculated and experimentally studied by quantum chemical calculation and liquid-liquid extraction process. The results showed [BPy][BF_4] have stronger interaction with toluene than that with cyclohexane. The selectivity of SILM processes was larger than 10 at the temperature of 323 K and the flow rate of 13.5 $mL \cdot min^{-1}$ on both shell side and lumen side. Due to the higher viscosity of IL, SILM process had good long-term stability. As the effects of mass transfer driving force of SILM process, the flux and removal efficiency increased with increase of initial toluene concentration, while the selectivity decreased because of the competitive transport. Base on the resistance in-series model and experimental results, the mass transfer resistance was mainly lay liquid membrane phase. The influence of flow rates on both sides was slight. The higher temperature could enhance the mass transfer performance significantly. The removal efficiency increased from 28.2% to 45.1% with the increasing of operation temperature from 298 K to 323 K.

Keywords: Supported Ionic Liquid Membrane, Separation, Toluene, Cyclohexane, Quantum Chemical Calculation

INTRODUCTION

With the development of the petrochemical industry, the demand for fuels and chemical raw materials is sharply increasing. To use naphtha efficiently, it is necessary to separate various fractions apart, and in which the separation of aromatics/aliphatic hydrocarbons system is considered as a significant step in the petroleum industry. However, it is quite challenging for conventional distillation [1] because they are apt to generate azeotrope [2] and the boiling points are fairly close to each other when they contain similar content of carbon.

Room temperature ionic liquids (ILs) have been extensively studied because they basically have no vapor pressure, low melting point, high viscosity, wide liquid range and high conductivity [3-5]. ILs can be designed due to the flexibility of physical and chemical properties through the judicious selection of cation and anion [6-8]. They are widely applied in many fields, such as organic synthesis, electrochemistry, extraction, catalysis for clean technology and liquid crystals. In recent year, ILs have been playing an important role in separation science [9].

The separation of aromatic/aliphatic hydrocarbons by liquid-liquid extraction with ILs has been studied in some papers. Pereiro et al. [10] studied the ternary liquid-liquid equilibrium among heptane, toluene and 1-buthyl-1-methylpyrrolidinium bis(trifluoromethanesulfon) imide([BMpyr][NTf_2]) at 298.15 K. The comparison between [BMpyr][NTf_2] and sulfolane demonstrated that IL was efficient solvent in the separation of aromatics from aliphatic hydrocarbons. Sundmacher et al. showed that 1-alkyl-3-methylimidazolium hexafluorophosphate([Cnmim][PF6]) was a promising solvent for benzene-cyclohexane extractive separation [11]. The distribution coefficient of benzene increases and solvent selectivity decreases with the length of cation alkyl chain growing.

Supported liquid membrane (SLM) is one of the three-phase liquid membrane systems. It is prepared by the intermolecular interaction and capillary action to make membrane phase solvents adsorbed in micropores. So it could facilitate the transport of target substances in feed phase to stripping phase. The SLM is preferred for its high mass transfer rate and good selectivity,but it is not stable due to the loss of the immobilized solvent. The membrane phase solvent can be dissolved or dispersed into adjacent phases. Many efforts have been made to enhance the stability of SLM [12-14]. Ren et al. studied hollow fiber renewal liquid membrane (HFRLM) technology for extraction of copper (II) from wastewater [15]. Because membrane phase solvent is renewed constantly during the process, the HFRLM process is very stable. Pancharoen et al. [16-18] investigated toxic metals separation and stripping through hollow fiber supported liquid membrane. They also studied the mathematical model and the results obtained from the model fitted well with that from the experimental results. The strong electrostatic interaction between ILs and polymeric materials can improve the stability of the membrane [9, 19]. The supported ionic liquid membrane (SILM), which combined SLM and ILs, was investigated in some process [20,21]. Chakraborty et al. [22] studied four ILs to separate aromatics and alkane mixture with n-dodecane as receiving phase. Their results showed that separation performance remained steady within 24 hr. The separation factor was over 15 and the removal efficiency of toluene was over 40%. Matsumoto et al. [23] stated that aromatic hydrocarbons were successfully transported through the SILM. The selectivity of

---

[†]To whom correspondence should be addressed.

E-mail: renzq@mail.buct.edu.cn

Table 1. Geometric parameters of membrane module

Effective length of module, L/m	Inner diameter of module, d_i/m	Inner diameter of fiber, $d\times10^{-3}$/m	Thickness of fiber, $\delta\times10^{-3}$/m	Packing factor
0.3	0.016	0.78	0.24	0.27

aromatic was improved to 67 while benzene was used as aromatic permeation. Some other researchers have reported that selective transportation of aromatic and aliphatic hydrocarbons was achieved by SILM through vapor permeation and gained good separation performance [24,25].

In recent years, theoretical quantum chemical calculations have been used as a complementarity for experimental methods in some fields to validate experiment results. The interaction between ILs and the system can be used to select appropriate ILs. Deetlefs et al. [26] studied the interactions between ILs and aromatic (benzene) were mainly attributed to the interaction forces of cations and aromatic ring. The study of Tsuzuki et al. [27,28] showed that the interaction in aromatic with alkyl pyridinium should be categorized into cation/π interaction.

In this paper, N-Butylpyridinium tetrafluoroborate ([BPy][BF_4]) and 1-Butyl-3-methylimidazoliumte trafluoroborate ([Bmim][BF_4]) were synthesized and tested for their low melting point, and low toxicity. At the same time they are quite appropriate for the SILM process because of relative low viscosity and cost. Toluene and cyclohexane were chosen as the representations of aromatics and alkane, and the quantum chemical calculation on the interactions of ILs with toluene and cyclohexane was conducted. IL was used as solvent in both liquid-liquid extraction and SILM process to separate toluene from cyclohexane. In SILM process, hollow fiber membrane was used as it can provide large specific surface area for mass transfer. The stability of the SILM process was tested for 100 h. Some parameters, such as the initial concentrate of toluene in feed phase, flow rates in two sides and process temperature, were also examined.

EXPERIMENTS

1. Materials

Toluene, n-dodecane and cyclohexane supplied by Beijing Chemical Plant, Beijing, China, were at analytical grade (>99.5%). Ethanol and n-octane of GC grade (>99.8%) were supplied by Tianjin Jinke fine chemical industry research institute, Tianjin, China. The materials were used without further purification.

The IL was synthesized and puried in our laboratory following the procedure of Noda [29]. Nuclear magnetic resonance (NMR) spectroscopy was used to ensure the purity of IL. ^{1}H-NMR ($CDCl_3$, δ/ppm relative to TMS): 9.68 (d, 2H, J=6.8 Hz), 8.45 (t, 1H, J=7.6 Hz), 8.10 (t, 2H, J=6.8 Hz), 4.96 (t, 2H, J=6.8 Hz), 1.97 (m, 2H, J=7.2 Hz), 1.34 (m, 2H, J=7.2 Hz), 0.87 (d, 2H, J=7.2 Hz). And it was subjected to vacuum and moderate temperature (T=323.15 K) for some days to remove the solvents and moisture residual. Karl Fischer Titrino and Haake Rheomix600P were used to determine the water content (<100 ppm) and viscosity, respectively.

2. Experiment Procedures

2-1. Liquid-liquid Extraction

10 mL ILs and 10 mL toluene/cyclohexane mixture was poured into an Erlenmeyer flask. The flask was then placed in an oil bath. The temperature of oil bath was kept constant and the deviation was maintained within 0.1 K. The initial concentration of toluene varied. The extractions were carried out under vigorous stirring to obtain equilibrium. Then, the mixture was allowed to settle for 2 hr to guarantee a complete split of the equilibrium phases. The samples of both layers were collected for analysis.

The distribution coefficient (D_i) and selectivity ($S_{tol/cyh}$) of extraction processes can be calculated as follows:

$$D_i = \frac{x_i^{IL}}{x_i^{raf}} \tag{1}$$

$$S_{tol/cyh,Ex} = \frac{D_{tol}}{D_{cyh}} \tag{2}$$

where x_i is the mole fraction of component i, IL and raf represent the IL phase and raffinate phase, respectively.

2-2. Supported Ionic Liquid Membrane

The polyvinylidene fluoride (PVDF) hollow fiber membranes had both excellent chemical stability in aromatic compounds and good affinity for ionic liquid. The additional information about hollow fiber modules is listed in Table 1.

The SILM was prepared at room temperature by impregnating porous film with ILs at least 30 min. The hollow fiber module was operated in a recycling mode, and the schematic of the process is shown in Fig. 1. In the SILM process, a jacket structure with hot water was used in membrane module for heat preservation. Both feed and stripping phase solution were heated at the same time. The effective area of the hollow fiber membrane module was 0.05 m^2 and the specific surface area was 3,159 m^2/m^3. The transport experi-

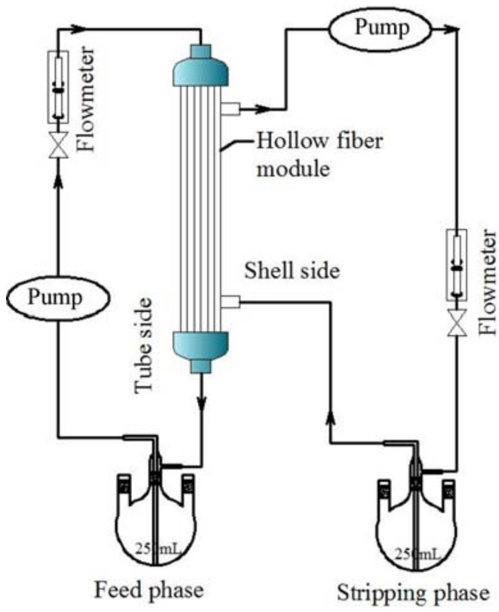

Fig. 1. The schematic layout of the SILM experiments.

ment was initiated by adding 150 mL of each solution into respective flask at room temperature. The mixture of toluene and cyclohexane flowed through the tube side, and n-dodecane flowed through the shell side countercurrently. Samples of both feed and stripping phases were withdrawn at regular time intervals.

The experimental mass transfer flux (J_f) of toluene transport across the SILM is defined by the following equation:

$$J_f=\frac{w}{A\Delta t} \tag{3}$$

where A is the membrane effective area, Δt is the time interval for sample collection, and w is the variations of toluene in mass in feed solution.

The separation factor ($S_{tol/cyh,LM}$) is defined as:

$$S_{tol/cyh,LM}=\frac{C^s_{tol}/C^s_{cyh}}{C^f_{tol}/C^f_{cyh}} \tag{4}$$

where C_{tol} and C_{cyh} are the concentrations of toluene and cyclohexane, respectively.

To indicate the influence of operating condition on the feed and the stripping phase, the removal efficiency of toluene based on feed phase is:

$$E=\frac{w}{C_0V_0}\times 100\% \tag{5}$$

where C_0 is the initial concentration of toluene in feed phase and V_0 is the initial volume of feed phase.

3. Analysis Method

The concentration of samples was determined by gas chromatography (GC) analysis with internal standard method, and n-octane was added to samples as an internal standard for GC. The concentration of toluene and cyclohexane in the samples was analyzed by

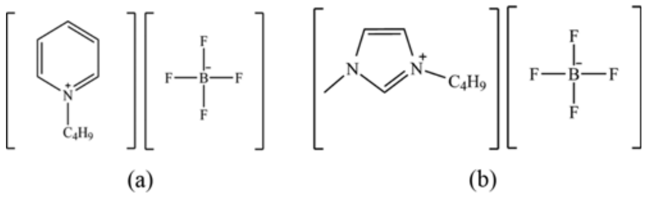

(a) (b)

Fig. 2. The structure of ionic liquids ((a) [BPy][BF_4]; (b) [Bmim][BF_4]).

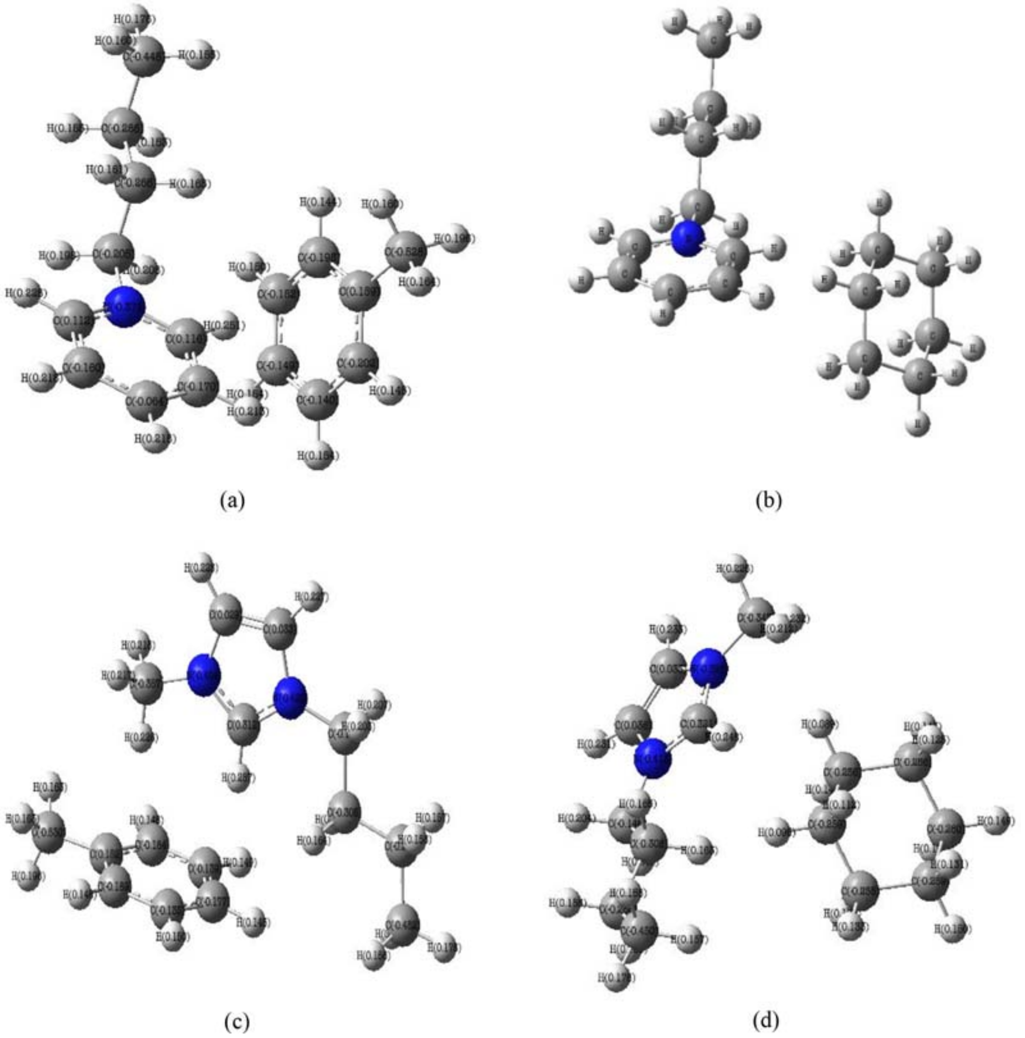

(a) (b) (c) (d)

Fig. 3. Optimized geometries of the complex of ILs and toluene, cyclohexane.

Agilent 7890A GC with a hydrogen flame ionization detector and 0.25 mm×30 m DB-FFAP capillary column, programmed temperature, injection and detector temperatures was 493 K and 523 K, respectively. Each analysis was carried out in duplicate to ensure accuracy.

RESULT AND DISCUSSION

1. Interactions of Toluene/Cyclohexane Mixtures with ILs

In this study, $[BPy][BF_4]$ and $[Bmim][BF_4]$ were synthesized and the structure is shown in Fig. 2. Quantum chemical calculations were conducted to characterize the preferred interaction sites between ILs and solvents. The calculations were performed by Gaussian 03 program. The B3LYP/6-31G* wave functions were selected as the input by using density functional theory to search for the minimum energy structure. The optimized geometries between ILs and solvents are shown in Fig. 3. It showed that the most stable geometries between ILs and solvents were obtained when the plane of solvents and cations were nearly vertical.

The interaction energy between $[BPy]^+$, $[Bmim]^+$ and toluene, cyclohexane is summarized in Table 2. The interaction energy between cations and toluene is much larger in magnitude than that between cations and cyclohexane. The difference of interaction between ionic liquid and solutes shows that the solubility of aromatic compounds in ILs is much larger than that of aliphatic compounds [28]. This is mainly because of the π-π interaction between cations of ILs and π bases compound (toluene). In the system of ILs and aromatic, the π-π interaction plays an important role due to the presence of many delocalized electrons. The difference of interaction between $[BPy]^+$ with the mixture of toluene and cyclohexane is larger than that of $[Bmim]^+$. Stronger interaction would lead to larger solubility and higher selectivity. So $[BPy]^+$ was used in our further experiments.

2. Liquid-liquid Extraction Process

The liquid-liquid extraction experiments were conducted at 298 K and 323 K for separation of toluene and cyclohexane with IL as extractant. The concentration range of toluene in cyclohexane was from 15 wt% to 90 wt%. The results are shown in Fig. 4. The distribution coefficient of toluene is higher than that of cyclohexane. With the increase of toluene concentration, the distribution coefficient of toluene increased from 0.21 to 0.25 at 293 K, and 0.22 to 0.27 at 323 K, respectively. And the distribution coefficient of cyclohexane increased from 0.02 to 0.09 at 293 K, and 0.03 to 0.16 at 323 K, respectively. But the separation factor of toluene decreased from 11.4 to 2.2 at 298 K, and 8.0 to 1.5 at 323 K as shows in Fig. 5, respectively. It is mainly because of the different solubility of toluene and cyclohexane in ILs. The extraction process is an equilibrium process and it is dominated by the physico-chemistry properties of the system. IL and toluene have the similar π-based structure; π-π interaction among the cation is the key factor for this system. The influence of temperature is slight [20]. As shown in section 3.1, the interaction energy of ILs-toluene is larger than that of ILs-cyclohexane. The experimental result is consistent with the quantum chemical calculation result.

Table 2. Interaction energies between ILs and toluene, cyclohexane

System	$\Delta E/kJ\cdot mol^{-1}$
$[BPy]^+$+toluene	−37.55
$[BPy]^+$+cyclohexane	−10.05
$[Bmim]^+$+toluene	−30.75
$[Bmim]^+$+cyclohexane	−7.37

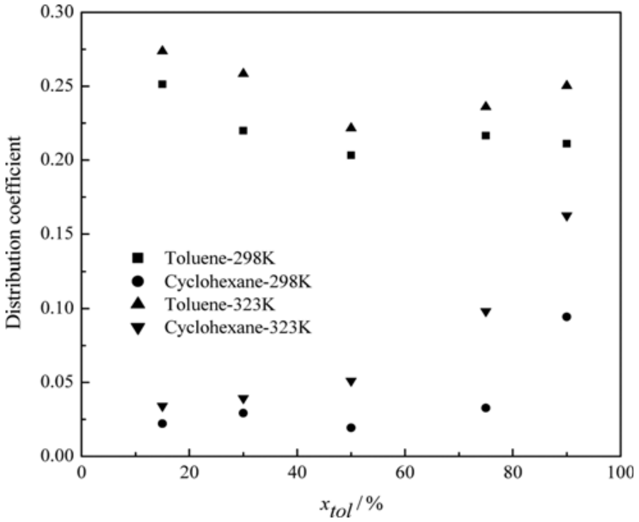

Fig. 4. Effect of initial concentration of toluene on distribution coefficients using $[BPy][BF_4]$ at 298 K and 323 K.

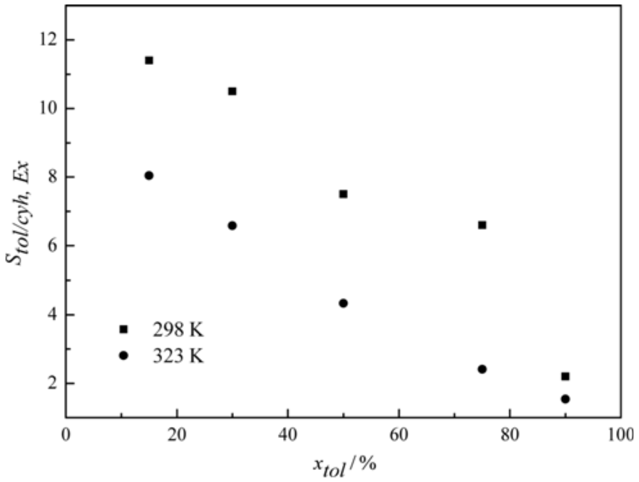

Fig. 5. Effect of temperature in raffinate on separation factor using $[BPy][BF_4]$.

3. Supported Ionic Liquid Membrane

3-1. Long-term Experiment of the Supported Ionic Liquid Membrane

The long-term stability is the key factor of SILM process. In this experiment, the initial concentration of toluene was 50 wt% and the temperature was 323 K. The flow rate was 13.5 $mL\cdot min^{-1}$ both on shell side and lumen side. The mass transfer driving force of process is the concentration difference between two sides of membrane. Continuous operation over 100 hr was conducted to test the stability of SILM. As shown in Fig. 6, the concentration of toluene between the tube and shell side is getting closer and closer, which are close to equilibrium value after 100 hr.

The equilibrium concentration of this process could be calcu-

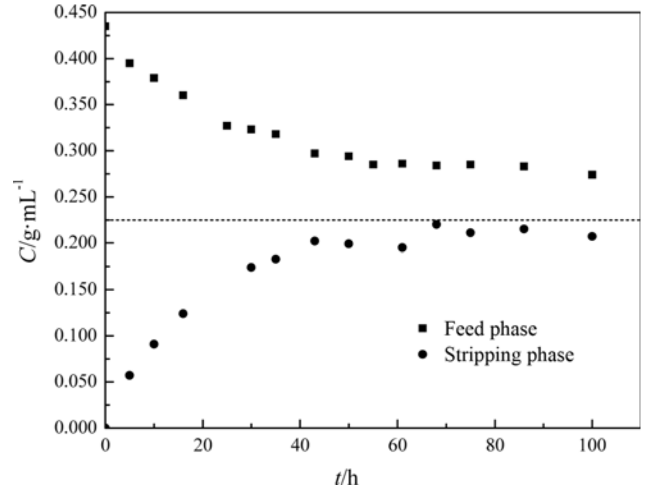

Fig. 6. Variation of the concentration of toluene in the feed and stripping solution in long-term stability experiment.

lated by Eqs. (6) and (7), as follows,

$$\frac{C_0V_f - nM}{V_f - nV_m} = \frac{nM}{V_s + nV_m} \tag{6}$$

$$C_e = \frac{nM}{V_s + nV_m} C_0 \tag{7}$$

Then the equilibrium concentration could be expressed,

$$C_e = \frac{V_f}{V_f + V_s} C_0 \tag{8}$$

where C_0 is the initial concentration of toluene, V_f is the volume of feed phase, V_m is the partial molar volume of toluene, V_s is the volume of stripping phase, M is the moles of toluene, and C_e is the equilibrium concentration.

According to above equations, the calculated equilibrium concentration (C_e) was half of the initial concentration (C_0), when the volume of feed phase and stripping phase was equal in our experiment. The concentration in stripping phase is close to C_e, while the value in feed phase is a little higher than C_e in Fig. 6. The experimental result was in good agreement with the calculated values. The experimental results also showed that the process was quite stable. It is mainly because of the higher viscosity of ILs than that of traditional solvents. The removal efficiency of toluene is over 80%, the average separation factor keeps over 10 during whole experiment. The experimental results indicate that SILM process can be used for the separation of toluene/cyclohexane.

3-2. Effect of Initial Concentration of Toluene in Feed Solution

The influence of initial concentration of toluene in feed phase on the mass transfer performance of SILM process was investigated at toluene concentration range from 15 wt% to 90 wt%. The operating temperature was 323 K, and the flow rates were 13.5 mL·min^{-1} both on shell side and lumen side. As shown in Fig. 7, the selectivity of [BPy][BF$_4$] increases from 5.0 to 11.5 with the decrease of toluene concentration in feed solution. However, the flux and re- moval efficiency of toluene increase with the increase of initial toluene concentration in feed phase as shown in Fig. 8. Actually, the transport of solute across SILM is a non-equilibrium process. The mass transfer driving force of toluene increases with the increase of toluene concentration in feed phase, which can enhance the transport of toluene, then more toluene was transported into membrane and stripping phase. The decrease of toluene in feed solution led to the increase of mass transfer driving force of cyclohexane. Then the flux of cyclohexane increased. It would reduce the separation factor of SILM process.

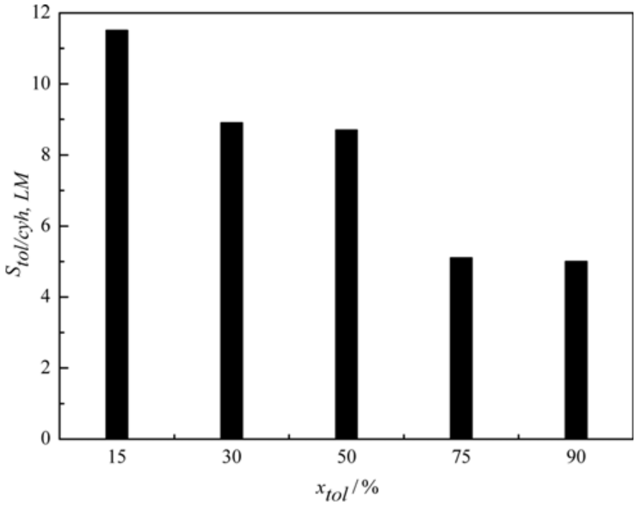

Fig. 7. Effect of initial concentration of toluene in feed solution on separation factor.

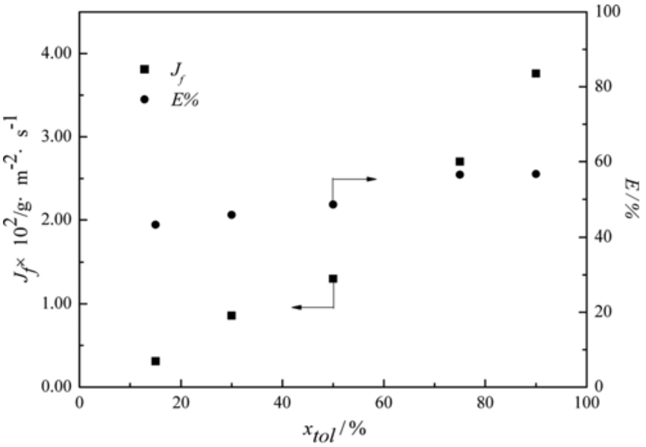

Fig. 8. Effect of initial concentration of toluene in feed solution on J_f and E% of toluene.

According to the literature [30], none of traditional processes showed favorable economics to manage feeds below 20 wt% of aromatics. The advantages of SILMs for these low aromatic content systems would be an alternative solution in industry.

3-3. Effect of Flow Rates in Two Sides

The flow rate has significant impact on the contact time and the thickness of liquid membrane layer. To study the mechanism of mass transfer in SILM process and determine the dominating part of mass transfer resistance, the flow rates in two sides of the SILM process were investigated. The initial concentration of toluene was 50 wt% and the temperature was 323 K. As shown in Fig. 9, the flux of toluene changes from 0.90×10^{-2} g·m^{-2}·s^{-1} to 1.19×10^{-2} g·m^{-2}·s^{-1} with the fluctuation of velocity in tube side. The same trend is obtained in

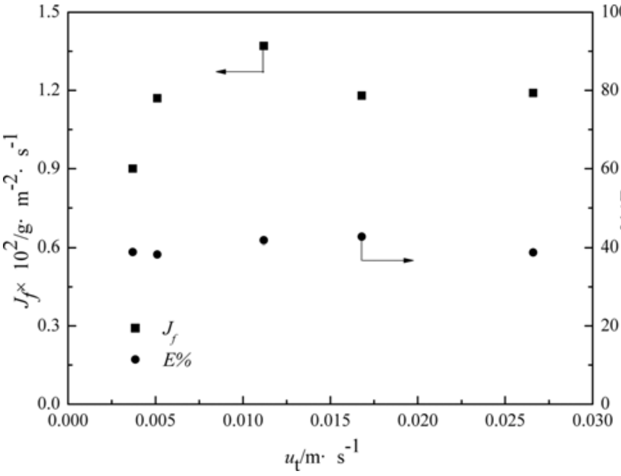

Fig. 9. Effect of flow rates of tube side on J_f and E% of toluene.

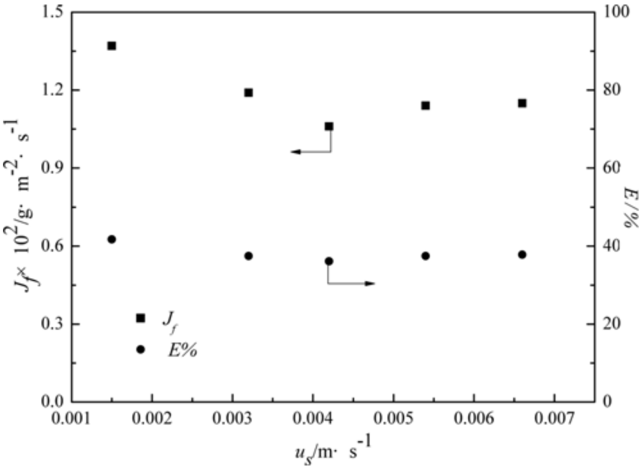

Fig. 10. Effect of flow rates of shell side on J_f and E% of toluene.

Fig. 10. The best separation performance was obtained when the velocity was 13.5 mL·min^{-1} both on shell side and lumen side.

To study the rate-controlling step in the transport of toluene through SILM, the fractional resistance of SILM process was calculated. In an SILM process, the overall mass transfer resistance is composed of the following individual mass transfer resistance, the resistance of layer diffusion in the tube side R_t, diffusion in the membrane phase R_m, and the layer diffusion in the shell side R_s. According to the resistance in-series theory and mass balance law, the overall mass transfer coefficient based on the feed phase in SILM process is [31],

$$\frac{1}{K_f}=\frac{1}{(k_{t,Toluene})}+\frac{1}{(mk_{m,Toluene})}+\frac{1}{mm'k_{s,Toluene}} \tag{9}$$

where K_f is the overall mass transfer coefficient, k is the individual mass transfer coefficient, m and m′ are distribution coefficients of extraction and back-extraction process, respectively.

The individual mass transfer coefficient in membrane phase, k_m, can be approximated according to [32]:

$$k_m=\frac{D_m\varepsilon}{\tau\cdot\delta} \tag{10}$$

where ε and τ are the porosity (0.85) and tortuosity (2.0) of membrane support, respectively.

D_m can be calculated by Wilke-Chang equation as follows:

$$D_m=\frac{7.4\times 10^{-8}(M_B)^{1/2}T}{\mu_B V_A^{0.6}} \tag{11}$$

where D_m is diffusion coefficient of toluene in [BPy][BF$_4$], cm^2/s, M_B is molecular weight of [BPy][BF$_4$], 223 g/mol; T is the temperature, V_A is the molar volume of toluene at its normal boiling temperature, 316 cm^3/mol; μ_B is the viscosity of [BPy][BF$_4$], the measured values was shown in Fig. 11.

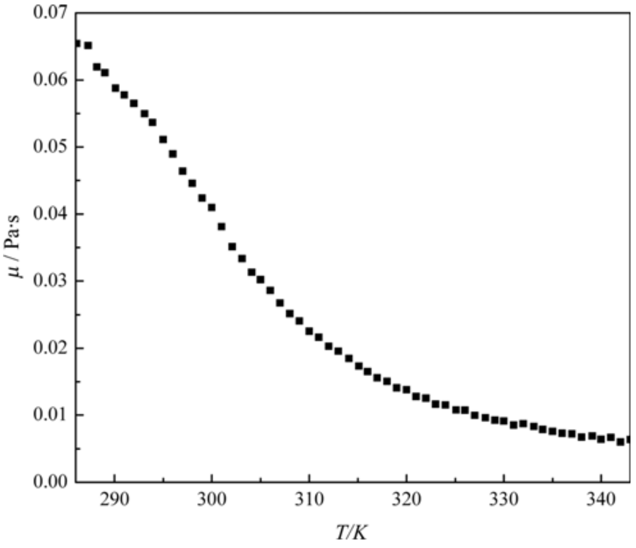

Fig. 11. Effect of temperature to the viscosity of [BPy][BF$_4$].

Table 3. Proportion of R_m in the overall mass transfer resistance

	298 K	323 K
k_m	4.14E-08	1.72E-07
R_m	1.05E08	2.65E07
K_f	9.37E-09	3.30E-08
$1/K_f$	1.07E08	3.03E07
Proportion/%	98	87

The calculated mass transfer resistances are listed in Table 3. The results showed that the mass transfer resistance mainly lay in membrane phase (98% at 298 K, 87% at 323 K). With the temperature increased, the proportion of diffusion resistance in membrane phase in overall mass transfer resistance decreased. The viscosity of IL decreased at high temperature as shown in Fig. 11. Then the diffusion coefficient of toluene and the mass transfer coefficient in membrane phase increased.

3-4. Effect of Temperature in SILM Process

As per above discussion, in an SILM process, the mass transfer resistance of diffusion across ionic liquid membrane phase is the controlling step. And the viscosity of ionic liquid has significant influence on the diffusion coefficient. The viscosity of ionic liquid is very sensitive to operating temperature. In this section, the operating temperature was investigated at 298 K and 323 K, and the results are shown in Fig. 12.

In stripping phase, the concentration of toluene increased more sharply at 323 K than that at 298 K. As listed in Table 4, the mass

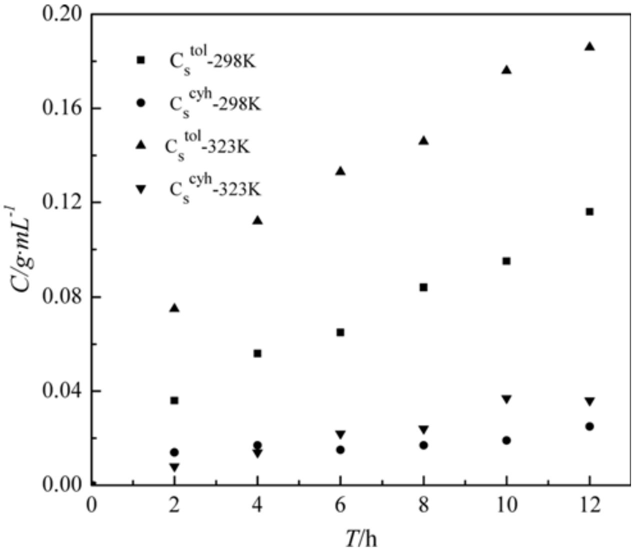

Fig. 12. Effect of temperature to the concentration of solvents in stripping phase.

Table 4. The effect of temperature in SILM process

T/K	E/%	$K_f \times 10^8/m\cdot s^{-1}$
298	28.2	0.94
323	45.1	3.30

transfer coefficient (K_f) was $3.30\times10^{-8}/(m\cdot s^{-1})$ at 323 K and $0.94\times10^{-8}/(m\cdot s^{-1})$ at 298 K.

As mentioned above, the liquid-liquid extraction process is an equilibrium transport process. But the SILM process is the coupling of extraction and back-extraction processes, a non-equilibrium transport process. The operating temperature could affect the transport rate of the SILM process, but not the equilibrium of extraction process. Therefore, in liquid-liquid extraction process, the influence of operating temperature was slight. But in the SILM process, higher temperature led to lower viscosity of ILs, which would enhance the diffusion coefficient of toluene in IL. It would increase the removal efficiency and mass transfer coefficient.

CONCLUSION

We used hollow fiber supported ionic liquid membrane process for the separation of toluene and cyclohexane with $[BPy][BF_4]$ as carrier. The quantum chemical calculations on the interactions of ionic liquids ($[BPy][BF_4]$ and $[Bmim][BF_4]$) with toluene and cyclohexane were conducted at B3LYP/6-31G* level. Based on the calculated and liquid-liquid extraction experimental results, the interaction energy between cations and toluene is much larger in magnitude than that between cations and cyclohexane. The distribution coefficient of toluene is higher than that of cyclohexane. The selectivity of ILs on toluene is over 11 when the initial concentration of toluene is 15 wt%. With the ionic liquid of $[BPy][BF_4]$ as membrane liquid, SILM process shows good long-term stability over 100 hr, depending on the higher viscosity of IL. The selectivity on toluene increased from 5.0 to 11.5 with the decrease of toluene concentration. The mass transfer flux of toluene changed from $0.90\times10^{-2}\ g\cdot m^{-2}\cdot s^{-1}$ to $1.19\times10^{-2}\ g\cdot m^{-2}\cdot s^{-1}$ and removal efficiency of toluene changed from 37.47% to 42.59% with the velocity fluctuation both in tube and shell side. The mass transfer resistance mainly lay in membrane phase. The higher operating temperature would lead to higher mass transfer performance of SILM. The results showed that SILM is an attractive method for the separation of toluene/cyclohexane.

ACKNOWLEDGEMENTS

This work was supported by the National Natural Science Foundation (No. 21076011 and 21276012), Program for New Century Excellent Talents in University (No. NCET-10-0210). The Authors gratefully acknowledge these grants.

NOMENCLATURE

a : specific surface area $[m^2\cdot m^{-3}]$
A : effective mass transfer area $[m^2]$
C : concentration $[g\cdot mL^{-1}]$
ΔC : driving force of mass transfer
d_i : inner diameter of module [m]
d : inner diameter of fiber [m]
D : distribution coefficient $[m^2\cdot s^{-1}]$
E : the removal efficiency of toluene
J : mass transfer flux $[g\cdot m^{-2}\cdot s^{-1}]$
k : individual mass transfer coefficient $[m\cdot s^{-1}]$
K : overall mass transfer coefficient based on the feed phase $[m\cdot s^{-1}]$
L : effective length of module [m]
m : distribution coefficient of extraction process
m′ : distribution coefficient of stripping process
M : molecular weight
R : the resistances of the layer diffusion
S : selectivity
Δt : time interval for sample collection
T : temperature
u : velocity $[m\cdot s^{-1}]$
V : volume $[cm^3]$
V_A : molar volume of toluene at its normal boiling temperature $[cm^3\cdot mol^{-1}]$
x : mole fraction
w : variations of toluene mass in the feed phase

Greek Letters

τ : tortuosity of hollow fiber membrane support
δ : Thickness of fiber, m
ε : porosity of hollow fiber membrane support
μ : viscosity $[Pa\cdot s]$

Subscript

cyh : cyclohexane
Ex : extraction
f : feed phase
LM : liquid membrane
m : membrane phase
s : shell side

st : stripping phase
t : tube side
tol : toluene

REFERENCES

1. U. Razdan, S. V. Joshi and V. Shah, *J. Curr. Sci.*, **85**, 761 (2003).
2. A. A. Gaile, G. D. Zalishchevskii, N. N. Gafur, L. V. Semenov, O. M. Varshavskii, N. P. Fedyanin and L. L. Koldobskaya, *Chem. Technol. Fuels Oils*, **40**, 215 (2004).
3. T. Welton, *Chem. Rev.*, **99**, 2071 (1999).
4. L. C. Branco, J. G. Crespo and C. A. Afonso, *Chem. Eur. J.*, **8**, 3865 (2002).
5. J. McFarlane, W. B. Ridenour, H. Luo, R. D. Hunt, D. W. DePaoli and R. X. Ren, *Sep. Sci. Technol.*, **40**, 1245 (2005).
6. E. R. Cooper, C. D. Andrews, P. S. Wheatley, P. B. Webb, P. Wormald and R. E. Morris, *Nature*, **430**, 1012 (2004).
7. R. Sheldon, *Chem. Commun.*, **23**, 2399 (2001).
8. H. Weingärtner, *Angew. Chem. Int. Ed. Eng.*, **47**, 654 (2008).
9. M. A. Malik, M. A. Hashim and F. Nabi, *Chem. Eur. J.*, **171**, 242 (2011).
10. A. B. Pereiro and A. Rodríguez, *AIChE J.*, **56**, 381 (2010).
11. T. Zhou, Z. Y. Wang, L. F. Chen, Y. M. Ye, Z. W. Qi, H. Freund and K. Sundmacher, *J. Chem. Thermodyn.*, **48**, 145 (2012).
12. X. J. Yang, A. G. Fane, J. Bi and H. J. Griesser, *J. Membr. Sci.*, **168**, 29 (2000).
13. Z. Q. Ren, W. D. Zhang, H. S. Li and W. Lin, *Chem. Eng. J.*, **146**, 220 (2009).
14. S. V. Ho, P. W. Sheridan and E. Krupetsky, *J. Membr. Sci.*, **112**, 13 (1996).
15. Z. Q. Ren, H. L. Meng and W. D. Zhang, *Sep. Sci. Technol.*, **44**, 1181 (2009).
16. S. Suren, T. Wongsawa, U. Pancharoen, T. Prapasawat and A. W. Lothongkum, *Chem. Eng. J.*, **191**, 503 (2012).
17. S. Suren, U. Pancharoen, N. Thamphiphit and N. Leepipatpiboon, *J. Membr. Sci.*, **448**, 23 (2013).
18. T. Wongsawa, N. Leepipatpiboon, N. Thamphiphit, U. Pancharoen and A. W. Lothongkum, *Chem. Eng. J.*, **222**, 361 (2013).
19. D. Han and K. H. Row, *Molecules*, **15**, 2405 (2010).
20. R. Fortunato, C. A. Afonso, M. A. M. Reis and J. G. Crespo, *J. Membr. Sci.*, **242**, 197 (2004).
21. Y. Y. Jiang, Z. Zhou, Z. Jiao, L. Li, Y. T. Wu and Z. B. Zhang, *J. Phys. Chem. B.*, **111**, 5058 (2007).
22. M. Chakraborty, D. Dobaria and P. A. Parikh, *Petro. Sci. Technol.*, **30**, 2504 (2012).
23. M. Matsumoto, Y. Inomoto and K. Kondo, *J. Membr. Sci.*, **246**, 77 (2005).
24. M. Matsumoto, K. Ueba and K. Kondo, *Desalination.*, **241**, 365 (2009).
25. B. Wang, J. Lin, F. Wu and Y. Peng, *Ind. Eng. Chem. Res.*, **47**, 8355 (2008).
26. M. Deetlefs, C. Hardacre, M. Nieuwenhuyzen, O. Sheppard and A. K. Soper, *J. Phys. Chem. B.*, **109**, 1593 (2005).
27. S. Tsuzuki, M. Mikami and S. Yamada, *J. Am. Chem. Soc.*, **129**, 8656 (2007).
28. S. Tsuzuki, M. Yoshida, T. Uchimaru and M. Mikami, *J. Phys. Chem. A.*, **105**, 769 (2001).
29. A. Noda and M. Watanabe, *Electrochim. Acta*, **45**, 1265 (2000).
30. A. Arce, M. J. Earle, H. Rodríguez and K. R. Seddon, *Green Chem.*, **9**, 70 (2007).
31. Z. Q. Ren, W. D. Zhang, Y. M. Liu, Y. Dai and C. H. Cui, *Chem. Eng. Sci.*, **62**, 6090 (2007).
32. R. M. C. Viegas, M. Rodríguez, S. Luque, J. R. Alvarez, I. M. Coelhoso and J. P. S. G. Crespo, *J. Membr. Sci.*, **145**, 129 (1998).